MICS JOURNAL

Mathematics-in-Industry Case Studies Journal, Volume 1, pp. 24-48 (2008)

Modelling the temperature, maturity and moisture content in a drying concrete block

T.G. Myers [*] J.P.F. Charpin [†]

Abstract. In this paper, the maturation of large concrete blocks is studied. A set of governing equations is presented, describing the one-dimensional variation of temperature, moisture and maturity of the concrete with time. The bottom of the block is in contact with the ground, and assumed to be insulated. The top exchanges heat with the surrounding air, whose temperature varies with time, it is also heated by solar radiation. A set of governing equations describing the one-dimensional variation of temperature, moisture and maturity of the concrete with time is presented. Non-dimensionalisation allows us to find a simple analytical solution, valid for short times. The full system of equations is also solved numerically. The analytical and numerical results show good agreement at first for short times but the numerical method must be used for longer times. Simulations are carried out for the periods of one day and two months. The effect of adding a second concrete block on top of the first one, at a later time, is also investigated.

Keywords. concrete, maturity, heat transfer

1 Introduction

When cement is mixed with water to form concrete, an exothermic reaction occurs. The heat generated by this reaction leads to thermal expansion of the concrete and consequently, when the concrete cools down it will contract and induce a stress in the material. If the stress is sufficiently large it can lead to cracking, which obviously impairs the quality of the structure. When the size of the structure is small, surface cooling can quickly remove the heat and the resultant stresses will not be large. However, with large amounts of concrete, surface cooling reduces the internal temperature slowly and the temperature increase can be large and over long time periods, high stresses can build up. For this reason large concrete structures, such as dams, are built sequentially. New layers are only added when the previous ones have cooled down and contracted sufficiently.

[*]Department of Mathematics and Applied Mathematics, University of Cape Town, Private Bag, Rondebosch 7701, South Africa, myers@maths.uct.ac.za

[†]MACSI, Department of Mathematics and Statistics, University of Limerick, Limerick, Ireland, jean.charpin@ul.ie

The build up of heat in a concrete block is caused by the concrete reacting with water. Therefore in order to model the temperature evolution in a concrete block, it is necessary to describe the water content (the moisture) as well as the proportion of cement available to react with the water (this is measured in terms of *maturity*). Knowledge of these variables is important for other reasons as well. If the water is used up before all the cement has reacted, the maturation process will end prematurely and the concrete does not reach its optimal strength. Pavlik *et al* [1] point out that the mould around a concrete block can only be removed after the concrete has reached a certain strength, which depends on the curing process. They describe a microwave technique for measuring water content as a means of determining the concrete maturity. West & Holmes [2] investigate the problem of damage to impervious concrete floor coverings. This problem arises because builders often do not wait for the concrete to dry properly before installing the floor. Further, current tests to determine when the floor can be installed only measure the concrete surface moisture content, not the moisture in the block.

An understanding of the temperature, moisture content and maturity of concrete is therefore important in determining when to add new layers. It also helps determine the strength of the concrete block and possibility of cracking. For these reasons, at the first and third South African Mathematics in Industry Study Groups, the problem of modelling this process was presented by the Cement & Concrete Institute (CCI) based in Midrand, Gauteng, South Africa, see [5, 6]. The temperature is seen as a key issue in concrete modelling, since this is the simplest quantity to measure and also, obviously, indicates the strength of the thermal stress. Consequently the CCI has presented two other problems related to the cooling of concrete structures at recent study groups [7, 9]. The first involved determining appropriate boundary conditions for the temperature and evaporation of water from a concrete surface [7]. The second involved analysing the effect of pumping cold water through a concrete block. This problem arises because of the need of builders to complete construction in as short a time as possible. If the heat is only removed at a free surface one may have to wait a long time before the next layer can be laid. For example, prior to the construction of the Hoover dam, engineers at the US Bureau of Reclamation estimated that if the dam were built in a single continuous pour, the concrete would require 125 years to cool to the ambient temperature and that the resulting stresses would have caused the dam to crack and fail [8]. Embedding pipes into the block allows cold water to be passed through and consequently increases heat removal. Results from the study described in Myers *et al* [9] showed that the key factors in the process were the spacing between the embedded pipes and the flux of water.

In this paper, we describe the maturity model developed at the second meeting [4]. In §2, we discuss the model equations and appropriate initial and boundary conditions. In §3, we write the problem in non-dimensional form and identify small parameters. This permits us to make simplifications that are used in §4 to produce simple analytical solutions. In §5, we describe a numerical scheme to solve the full system of equations. Results are presented for simulations over the periods of one day and two months. We also examine the effect of adding a second concrete

block at a later time, e.g., after one month.

2 Model equations

The mathematical model of the maturation process involves three coupled equations:

$$\rho_c c_c \frac{\partial T}{\partial t} = \kappa_c \frac{\partial^2 T}{\partial x^2} + \frac{\partial Q}{\partial t} , \tag{1}$$

$$\frac{\partial m}{\partial t} = \mu(1-m)\theta e^{-E/RT} , \tag{2}$$

$$\frac{\partial \theta}{\partial t} = \frac{\partial}{\partial x}\left(D(\theta)\frac{\partial \theta}{\partial x}\right) - \eta \frac{\partial m}{\partial t} , \tag{3}$$

where T, m and θ denote the temperature, maturity and moisture of the concrete respectively. All notation and typical parameter values are defined in the nomenclature section, §7. Equation (1) is the standard heat equation with a source term due to the chemical reaction. Ballim and Graham [3] have shown that rate of heat evolution may be expressed in terms of the maturity. Hence we may write $\partial_t Q = Q_m \partial_t m$; a typical plot for $Q(t)$ is presented in [9]. The form of Q_m is discussed in [3], where it is shown to have an initial sharp rise followed by a slow decay, hence, for the present work we will use the approximation of [4]

$$Q_m = Ame^{-am^2} . \tag{4}$$

If the maximum value of Q_m occurs at (m_x, Q_x), where m_x and Q_x are measurable quantities, then $a = 1/2m_x^2$, $A = Q_x\sqrt{e}/m_x$. The maturity is a measure of the amount of cement that has reacted with the water and is described by an Arrhenius type equation, Equation (2). Finally, the water content or moisture must also satisfy a diffusion equation. The sink term, $-\eta\partial_t m$, is the rate of water used up in the reaction.

All coefficients in (1)–(3) are approximately constant throughout the reaction, with the exception of the diffusion coefficient, $D(\theta)$, which varies with the moisture. This variation is discussed by West *et al* [2]. Their results are well represented by the relation

$$D(\theta) = D_m\left[\alpha + (1-\alpha)\left(1 + \tanh a(\theta - \theta_m)\right)\right] \tag{5}$$

where $D_m \sim 2 \times 10^{-9}\mathrm{m}^2/\mathrm{s}$, $\alpha \sim 0.05$, $\theta_m \sim 0.8$ and $a \sim 20$.

In the following work we will take D as constant $D \sim 2\times10^{-9}\mathrm{m}^2/\mathrm{s}$ when doing calculations using analytical results. In the numerical computations we will allow for diffusion variation according to Equation (5).

The initial water content, θ_s, and temperature, T_s, are assumed known and constant to be constants. The initial maturity must be zero, hence suitable initial conditions are

$$m(x,0) = 0 \ , \quad \theta(x,0) = \theta_s \ , \quad T(x,0) = T_s \ .$$

At the free surface, $x = L$, a cooling condition applies [6]

$$-\kappa_c \frac{\partial T}{\partial x} = -Q_s + H(T - T_a) \ , \tag{6}$$

where Q_s represents the solar radiation and T_a the ambient temperature. Both can be functions of time, for example

$$T_a(L,t) = T_s + T_d \cos \omega_d t \tag{7}$$

reflects the daily temperature variation, where $T_s = (T_{max} + T_{min})/2$ is the average temperature during the day and $T_d = T_{max} - T_{min}$.

It was shown [7] that the concrete surface temperature lags behind the air temperature and is also greatly affected by the solar radiation (in agreement with experimental measurements).

Since evaporation occurs at the free surface, the moisture boundary condition is

$$-D(\theta(L,t)) \left. \frac{\partial \theta(x,t)}{\partial x} \right|_{x=L} = \overline{e}(\theta_a - \theta(L,t)) \ . \tag{8}$$

West *et al* [2] also discuss the evaporation rate $\overline{e}$ in equation (8). This rate actually decreases slowly with time, however, the change, in a controlled room, is around 5% after 50 days. In the lab the decrease is around 17% after 90 days, hence in the following we will treat it as constant, $\overline{e} \sim 1.8 \times 10^{-9}$ m/s.

Finally, we assume that the bottom of the block is insulated. This could represent a block on soil or other relatively poor conductor. However, the block could be on top of rock which is a good conductor and in that case a different condition will be required. In the absence of information concerning the base, we choose the insulated condition.

3 Non-dimensional equations

The variables are non-dimensionalised in the following manner

$$\hat{x} = \frac{x}{L} \ , \quad \hat{t} = \frac{t}{\tau} \ , \quad \hat{T} = \frac{T - T_s}{\Delta T} \ , \quad \hat{D} = \frac{D}{D_m} \ , \quad \hat{Q}_m = \frac{Q_m}{Q_x} \ ,$$

where τ and ΔT are the, as yet, unspecified time and temperature scales. The maturity and moisture content are fractions between 0 and 1 and already non-dimensional. We drop the hat for ease of notation.

The heat equation (1) becomes

$$\frac{\partial T}{\partial t} = \frac{\kappa_c \tau}{\rho_c c_c L^2}\frac{\partial^2 T}{\partial x^2} + \frac{Q_x}{\rho_c c_c \Delta T} Q_m \frac{\partial m}{\partial t} \ . \tag{9}$$

The maturity equation (2) may be written as

$$\frac{\partial m}{\partial t} \ = \ \tau \mu e^{-\lambda}(1-m)\theta \exp\left[\lambda\left(1 - \frac{T_s + \Delta T}{T_s + \Delta T\ T}\right)\right] \tag{10}$$

where $\lambda = E/[R(T_s + \Delta T)]$. We assume that the temperature variation is due to the exothermic reaction and choose a temperature scale based on the source term in the heat equation

$$\Delta T = \frac{Q_x}{\rho_c c_c} \approx 48.3\text{K} \ .$$

From these equations we have two choices for time-scale, coming either from the temperature diffusion term or the maturity equation,

$$\tau_T \ = \ \frac{\rho_c c_c L^2}{\kappa_c} \approx 1.36 \times 10^7 s \approx 157 \text{ days}$$

or

$$\tau_m \ = \ \frac{1}{\mu}\exp(\lambda) \approx 2.08 \times 10^5 s \approx 2.4 \text{ days} \ .$$

Another time-scale comes from the moisture diffusion, $\tau_D = 4.5 \times 10^9$s $\approx$ 140 years. This indicates the moisture movement is extremely slow and it is essential to start the process with the correct amount of water.

Working on the faster time-scale, τ_m, the non-dimensional governing equations become

$$\frac{\partial T}{\partial t} \ = \ \alpha_1 \frac{\partial^2 T}{\partial x^2} + Q_m \frac{\partial m}{\partial t}, \tag{11}$$

$$\frac{\partial m}{\partial t} \ = \ (1-m)\theta \exp\left[\lambda\left(1 - \frac{T_s + \Delta T}{T_s + \Delta T\ T}\right)\right], \tag{12}$$

$$\frac{\partial \theta}{\partial t} \ = \ \alpha_2 \frac{\partial}{\partial x}\left(D(\theta)\frac{\partial \theta}{\partial x}\right) - \eta \frac{\partial m}{\partial t}, \tag{13}$$

where

$$\alpha_1 = \frac{\kappa_c \tau}{\rho_c c_c L^2} \approx 0.015 \ , \ \alpha_2 = \frac{D_m \tau}{L^2} \approx 4.6 \times 10^{-5} \ , \ \lambda = \frac{E \rho_c c_c}{R\left(Q_x + \rho_c c_c T_s\right)} \approx 12.2 \tag{14}$$

and

$$Q_m = \frac{m}{m_x} e^{(1 - m^2/m_x^2)/2} \ . \tag{15}$$

The corresponding boundary conditions are:

At $t = 0$

$$T(x,0) = 0 \ , \qquad m(x,0) = 0 \ , \qquad \theta(x,0) = 1 \ . \tag{16}$$

At $x = 0$

$$\left.\frac{\partial T}{\partial x}\right|_{x=0} = 0 \ , \qquad \left.\frac{\partial \theta}{\partial x}\right|_{x=0} = 0 \ . \tag{17}$$

At $x = 1$, flux conditions are imposed for temperature and moisture

$$\left.\frac{\partial T}{\partial x}\right|_{x=1} = \beta_1 - \beta_2 \, T|_{x=1} \ , \qquad \left.\left(D(\theta)\frac{\partial \theta}{\partial x}\right)\right|_{x=1} = -\beta_3 \left(\theta|_{x=1} - \theta_a\right) \ , \tag{18}$$

where the constants β_1, β_2 and β_3 are defined by

$$\beta_1 = \frac{Q_s L - HL\,(T_s - T_a)}{\kappa_c \Delta T} \ , \quad \beta_2 = \frac{HL}{\kappa_c} \ , \quad \beta_3 = \frac{L\bar{e}}{D_m} \ . \tag{19}$$

Since the ambient temperature, T_a, varies with time $\beta_1 = \beta_1(t)$. The constant $\beta_2 \approx 10$, which may lead to high gradients near the boundary and indicates the presence of a boundary layer there, and the final constant $\beta_3 = 2.7$.

4 Solutions in the bulk

We begin our analysis by looking at a simplified system that holds in the bulk. Now consider the parameter values shown in Equation (14). The diffusion parameters α_1 and α_2 are both small. Physically this means diffusion is, in general, slow and consequently the x variation of T and θ is negligible throughout most of the domain. Neglecting the x derivatives means we are unable to satisfy the boundary conditions. Since we choose $T_x = \theta_x = 0$ at the bottom, an x independent solution is automatically satisfied there, however, to satisfy the upper conditions a boundary layer must be present in the vicinity of $x = 1$.

A standard boundary layer scaling indicates the appropriate thermal and moisture layer thicknesses are given by $L_T = \sqrt{\alpha_1}$ and $L_m = \sqrt{\alpha_2}$ respectively. Using the values given in Equation (14) we expect $L_T \approx 1$cm, $L_m \approx 0.5$mm. However, in general, the fluctuations in the ambient temperature prevents us from seeing the boundary layer. We also see no benefit in carrying out the boundary layer analysis since when we rescale in the boundary layers we end up retaining all terms in the governing equations, even the original boundary conditions hold. Instead we will now simply examine the solution in the bulk.

Neglecting the small diffusion terms our temperature and moisture equations are

$$\frac{\partial T}{\partial t} = Q_m \frac{\partial m}{\partial t} \ , \qquad \frac{\partial \theta}{\partial t} = -\eta \frac{\partial m}{\partial t} \ . \tag{20}$$

The second equation integrates immediately to determine the moisture in terms of the maturity

$$\theta = 1 - \eta m \ . \tag{21}$$

So the moisture decreases linearly with maturity. With the definition of Q_m given by Equation (15) we find

$$T = m_x\sqrt{e}\left(1 - e^{-m^2/(2m_x^2)}\right) \ . \tag{22}$$

At this stage we can use these expressions to replace T and θ in the moisture equation, leaving a first order differential equation to solve numerically and hence determine the bulk solution for m. Alternatively we may note that the exponential term in the maturity equation contains $1 - (T_s + \Delta T)/(T_s + \Delta T\ T)$. Provided T remains small, $1 - (T_s + \Delta T)/(T_s + \Delta T\ T) \approx -\Delta T/T_s$. Hence a reasonable approximation to the maturity equation is

$$\frac{\partial m}{\partial t} \quad = \quad (1-m)\theta e^{-\bar{\lambda}} \ , \tag{23}$$

where

$$\bar{\lambda} = \lambda\frac{\Delta T}{T_s} = \frac{E}{RT_s}\frac{Q_x}{\rho_c c_c T_s + Q_x} \approx 2 \ .$$

Substituting for θ in (23) leads to a first order separable equation for m,

$$\frac{\partial m}{\partial t} = (1-m)(1-\eta m)e^{-\bar{\lambda}} \ . \tag{24}$$

The solution is

$$m = \frac{1 - e^{e^{-\bar{\lambda}}(\eta-1)t}}{1 - \eta e^{e^{-\bar{\lambda}}(\eta-1)t}} \ . \tag{25}$$

In the case $\eta = 1$ we find the solution

$$m = \frac{te^{-\bar{\lambda}}}{1 + te^{-\bar{\lambda}}} \ . \tag{26}$$

The corresponding solutions for the moisture, θ are

$$\theta = 1 - \eta\frac{1 - e^{e^{-\bar{\lambda}}(\eta-1)t}}{1 - \eta e^{e^{-\bar{\lambda}}(\eta-1)t}} \tag{27}$$

and, in the limiting case $\eta = 1$,

$$\theta = 1 - \frac{te^{-\bar{\lambda}}}{1 + te^{-\bar{\lambda}}} \ . \tag{28}$$

For the present study we take $\eta = 1.25$ and so as $t \to \infty$ the maturity $m \to 1/\eta$ while the moisture content $\theta \to 0$. The maximum value of T is independent of η and $T \to m_x\sqrt{e} \sim 0.247$. These limits may be observed in Figure 1, which shows solutions for m, θ and T given by equations (22), (25), and (27) as dashed lines. The solid lines are the corresponding results obtained by solving the original differential equation for m, Equation (12), with T and θ taken from equations (21), and (22). The time-scale is $\tau = 2.08 \times\ 10^5$s, so this simulation which runs to $t \approx 20$, corresponds

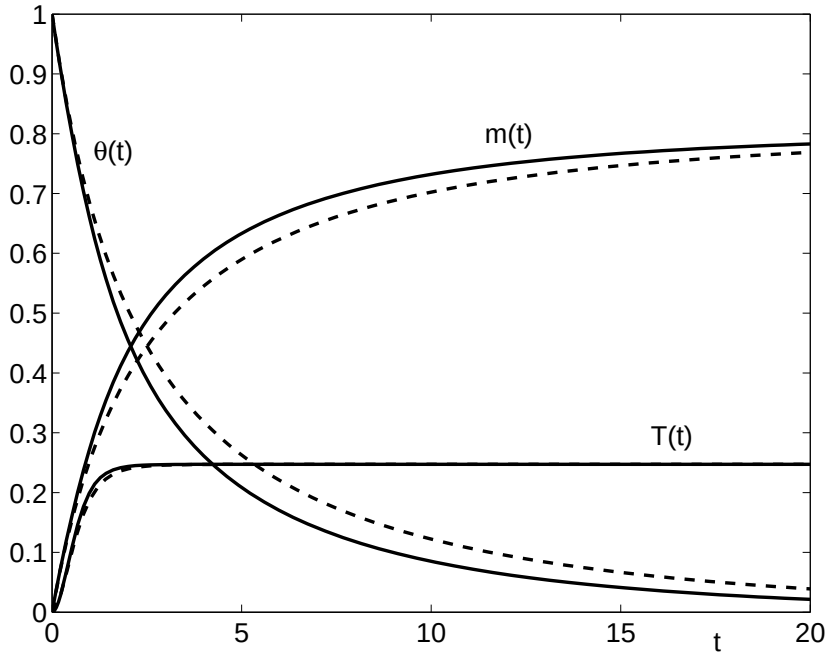

Figure 1: *Variation of m, θ and T with time.*

to 50 days. In all cases, we see that the simple solution is very close to the numerical solution, particularly in the case of the temperature. The maturity increases monotonically, tending to the asymptote $1/\eta$=0.8. After 50 days it is close to this value at $m \sim 0.77$. The moisture θ decreases as m increases. The temperature also increases towards an asymptote. With the present temperature scale $\Delta T = 48.3$K this corresponds to a rise of only 12K. Due to the exponential decay of T with m in equation (22) it should be expected that T only varies for small times. This has consequences for the neglect of the term involving T in the maturity equation. To simplify the maturity equation, we set $T \approx 0$. When $T \sim 0.25$, we may expect a significant error in this approximation and since T builds up rapidly the approximation can only hold for short time periods, of the order of days. We verify this in subsequent graphs in §5. In particular, in Figure 6, we show that the maturity approximation is excellent after 2 days with only a small difference at the surface. After 10 days there is a 15% difference between analytical and numerical bulk solutions

In general, of the three sets of curves, we expect the temperature to be the least realistic. The maturity satisfies a first order ordinary differential equation, and we satisfy the initial condition. The temperature and moisture both satisfy diffusion equations. When we neglect the diffusion terms, we satisfy the initial condition and the boundary condition at $x = 0$, but not the surface condition at $x = 1$. Since the coefficient $\alpha_2 \ll \alpha_1$, we expect the largest boundary layer effect in the temperature equation. Hence we expect the best approximation for m, and the worst for T. We will investigate this further when we solve the full equations numerically in §5.

From these results we can make a statement about η. Firstly, if $\eta > 1$ then as $t \to \infty$ the

exponential terms dominate in (25) and $m \to 1/\eta$. Hence the maturity can never reach unity. If $\eta < 1$ then as $t \to \infty$ the exponential terms decay and the maturity $m \to 1$. If $\eta = 1$ we also find $m \to 1$. Experimental results show that the maturity typically increases to a maximum of around $m = 0.8$. This motivates our choice $\eta = 1.25$. In practice by taking a number of maturity measurements over time, we could estimate both parameters, λ and η, in the maturity equation.

5 Numerical method and solutions

5.1 Numerical scheme

The system (11)-(19) will now be solved numerically, using a standard finite difference method. The three variables T, m and θ are calculated on equally spaced points numbered from 0 to n_x, including the boundaries, separated by the space step $\Delta x = 1/n_x$. The simulation time t_m is divided in n_t time steps denoted $\Delta t = t_m/n_t$. The temperature, maturity and moisture at $x = i\Delta x$ and $t = k\Delta t$ are denoted T_s^k, m_i^k, θ_i^k respectively.

To slightly simplify the system, the equations may be rewritten

$$\frac{\partial T}{\partial t} = \alpha_1 \frac{\partial^2 T}{\partial x^2} + Q_m(m)(1-m)\theta \exp\left[\lambda\left(1 - \frac{T_s + \Delta T}{T_s + \Delta T\ T}\right)\right] , \tag{29}$$

$$\frac{\partial m}{\partial t} = (1-m)\theta \exp\left[\lambda\left(1 - \frac{T_s + \Delta T}{T_s + \Delta T\ T}\right)\right] , \tag{30}$$

$$\frac{\partial \theta}{\partial t} = \alpha_2 \frac{\partial}{\partial x}\left(D(\theta)\frac{\partial \theta}{\partial x}\right) - (1-m)\theta \exp\left[\lambda\left(1 - \frac{T_s + \Delta T}{T_s + \Delta T\ T}\right)\right] . \tag{31}$$

Equations (29) and (31) are diffusion equations with respectively a source and a sink term. They involve second order space derivatives that are key to the stability of the numerical scheme. They will be discretised with a partially implicit scheme:

- The space derivatives are discretised using an implicit method to guarantee good stability of the numerical scheme,
- The two parameters, $D(\theta)$ and $Q_m(m)$, and the source and sink terms are discretised with an explicit method.

Equation (30) does not involve any space derivative and may be discretised using an explicit method.

The detailed description is given below.

Temperature

In general we use

$$-\left[\frac{2\alpha_1\Delta t}{\Delta x^2}\right]T_{i+1}^{k+1}+\left[1+\frac{2\alpha_1\Delta t}{\Delta x^2}\right]T_i^{k+1}-\left[\frac{2\alpha_1\Delta t}{\Delta x^2}\right]T_{i-1}^{k+1} = T_i^k+\Gamma_i\Delta t\ , \tag{32}$$

where

$$\begin{aligned}\Gamma_i &= \frac{1}{2}\left\{(1-m_{i-1/2})Q_m(m_{i-1/2})\theta_{i-1/2}\exp\left[\lambda\left(1-\frac{T_s+\Delta T}{T_s+\Delta T\ T_{i-1/2}}\right)\right]\right.\\ &\left.+(1-m_{i+1/2})Q_m(m_{i+1/2})\theta_{i+1/2}\exp\left[\lambda\left(1-\frac{T_s+\Delta T}{T_s+\Delta T\ T_{i+1/2}}\right)\right]\right\}\ ,\end{aligned}$$

$$T_{i+1/2}=\frac{T_i+T_{i+1}}{2}\ ,\quad m_{i+1/2}=\tfrac{m_i+m_{i+1}}{2}\ ,\quad \theta_{i+1/2}=\frac{\theta_i+\theta_{i+1}}{2}$$

for $1\le i\le n_x-1$.

At the boundary $x=0$, we apply $\partial_x T=0$ and so impose

$$\left[1+\frac{2\alpha_1\Delta t}{\Delta x^2}\right]T_0^{k+1}-\left[\frac{2\alpha_1\Delta t}{\Delta x^2}\right]T_1^{k+1} = T_0^k+\Gamma_0\Delta t\ . \tag{33}$$

At $x=1$, we apply (18) and set

$$-\left[\frac{2\alpha_1\Delta t}{\Delta x^2}\right]T_{n_x-1}^{k+1}+\left[1+\frac{2\alpha_1\Delta t}{\Delta x^2}+\frac{2\alpha_1\beta_2\Delta t}{\Delta x}\right]T_{n_x-1}^{k+1} = T_{n_x}^k+\frac{2\alpha_1\beta_1\Delta t}{\Delta x}+\Gamma_n\Delta t\ , \tag{34}$$

where

$$\begin{aligned}\Gamma_0 &= \frac{1}{2}\left\{(1-m_0)Q_m(m_0)\theta_0\exp\left[\lambda\left(1-\frac{T_s+\Delta T}{T_s+\Delta T\ T_0}\right)\right]\right.\\ &\left.+(1-m_{1/2})Q_m(m_{1/2})\theta_{1/2}\exp\left[\lambda\left(1-\frac{T_s+\Delta T}{T_s+\Delta T\ T_{1/2}}\right)\right]\right\}\end{aligned} \tag{35}$$

and

$$\Gamma_{n_x} = \frac{1}{2}\left\{(1-m_{n_x-1/2})Q_m(m_{n_x1/2})\theta_{n_x-1/2}\exp\left[\lambda\left(1-\frac{T_s+\Delta T}{T_s+\Delta T\ T_{n_x-1/2}}\right)\right]\right. \tag{36}$$

$$\left.+(1-m_{n_x})Q_m(m_{n_x})\theta_{n_x}\exp\left[\lambda\left(1-\frac{T_s+\Delta T}{T_s+\Delta T\ T_{n_x}}\right)\right]\right\}\ . \tag{37}$$

Maturity

$$m_i^{k+1}=m_i^k+\Delta t(1-m_i^k)\theta_i^k\exp\left[\lambda\left(1-\frac{T_s+\Delta T}{T_s+\Delta T\ T_i}\right)\right] \tag{38}$$

for $0\le i\le n_x$.

Moisture

In general we use

$$
\begin{aligned}
-\left[\frac{2\alpha_2\Delta t}{\Delta x^2}D\left(\theta^k_{i+1/2}\right)\right]\theta^{k+1}_{i+1} \\
+\left[1+\frac{2\alpha_2\Delta t}{\Delta x^2}\left(D\left(\theta^k_{i+1/2}\right)+D\left(\theta^k_{i-1/2}\right)\right)\right]\theta^{k+1}_{i} \\
-\left[\frac{2\alpha_2\Delta t}{\Delta x^2}D\left(\theta^k_{i-1/2}\right)\right]\theta^{k+1}_{i-1}=\theta^k_i+\eta\Lambda_i\Delta t\ ,
\end{aligned}
\tag{39}
$$

where

$$
\begin{aligned}
\Lambda_i &= \frac{1}{2}\left\{(1-m_{i-1/2})\theta_{i-1/2}\exp\left[\lambda\left(1-\frac{T_s+\Delta T}{T_s+\Delta T\ T_{i-1/2}}\right)\right]\right. \\
&\left.+(1-m_{i+1/2})\theta_{i+1/2}\exp\left[\lambda\left(1-\frac{T_s+\Delta T}{T_s+\Delta T\ T_{i+1/2}}\right)\right]\right\}
\end{aligned}
$$

for $1\le i\le n_x-1$.

At $x=0$, we apply $\partial_x\theta=0$ and so impose

$$
\begin{aligned}
\left[1+\frac{2\alpha_2\Delta t}{\Delta x^2}D\left(\theta^k_{1/2}\right)\right]\theta^{k+1}_0 \\
-\left[\frac{2\alpha_2\Delta t}{\Delta x^2}D\left(\theta^k_{3/2}\right)\right]\theta^{k+1}_1=\theta^k_0+\eta\Lambda_0\Delta t\ .
\end{aligned}
\tag{40}
$$

At $x=1$, we apply (18) and set

$$
\begin{aligned}
-\left[\frac{2\alpha_2\Delta t}{\Delta x^2}D\left(\theta^k_{n_x-1/2}\right)\right]\theta^{k+1}_{n_x-1} \\
+\left[1+\frac{2\alpha_2\Delta t}{\Delta x^2}D\left(\theta^k_{n_x-1/2}\right)-\frac{2\alpha_2\beta_3\Delta t}{\Delta x}\right]\theta^{k+1}_{n_x-1} \\
=\theta^k_{n_x}+\frac{2\alpha_2\beta_3\theta_a\Delta t}{\Delta x}D\left(\theta^k_{n_x}\right)+\eta\Lambda_n\Delta t\ ,
\end{aligned}
\tag{41}
$$

where

$$
\begin{aligned}
\Lambda_0 &= \frac{1}{2}\left\{(1-m_0)\theta_0\exp\left[\lambda\left(1-\frac{T_s+\Delta T}{T_s+\Delta T\ T_0}\right)\right]\right. \\
&\left.+(1-m_{1/2})\theta_{1/2}\exp\left[\lambda\left(1-\frac{T_s+\Delta T}{T_s+\Delta T\ T_{1/2}}\right)\right]\right\}
\end{aligned}
$$

and

$$
\begin{aligned}
\Lambda_{n_x} &= \frac{1}{2}\left[(1-m_{n_x-1/2})\theta_{n_x-1/2}\exp\left[\lambda\left(1-\frac{T_s+\Delta T}{T_s+\Delta T\ T_{n_x-1/2}}\right)\right]\right. \\
&\left.+(1-m_{n_x})\theta_{n_x}\exp\left[\lambda\left(1-\frac{T_s+\Delta T}{T_s+\Delta T\ T_{n_x}}\right)\right]\right\}\ .
\end{aligned}
$$

Equation (38) leads directly to the maturity at time $t = (k+1)\Delta t$. Equations (32)–(34) and (39)–(41) form two tri-diagonal systems of n_x linear equations for $2n_x$ unknowns, namely the values of T and θ at time $t = (k+1)\Delta t$. These two systems may be solved easily with an LU factorisation for example.

5.2 Numerical solutions

The solutions of the governing equations will be described in three different situations. Firstly the evolution of the variables for a short time period (a single day) will be studied, to evaluate the influence of the varying ambient conditions. Secondly, a simulation for a longer time period (two months) will be carried out, where a 3m concrete layer is built in a single stage. Finally, another simulation for a two-month time period will be studied where a 6m block is built in two stages, with the second stage being added after a one-month time period. This is compared with a 6m block built in a single stage. The values of the constants used for all simulations may be found in the nomenclature section, §7.

Temperature variation and sun exposure is represented as follows:

- Sunrise and sunset occur every day at 06.30 and 19.30 respectively.
- The minimum temperature $T_{min} = 288$K occurs one hour before sunrise.
- The maximum temperature is $T_{max} = 303$K.
- Temperature variation during the day is modelled with a cosine function.

Using the definition given in Equation (19), the parameter β_1 may then be expressed as

$$\beta_1 = 22.7 f(t) - 3.4 \cos\left[\frac{2\pi}{24}\left(\frac{\tau_m t}{3600} - 5.5\right)\right] ,$$

where t represent the time of the day in hours and the function $f(t)$ defines the daylight hours, when solar radiation plays a role,

$$f(t) = \begin{cases} 1 & \text{if} \quad 6.5 + 24n_d \leq 12 + \tau_m t/3600 \leq 19.5 + 24n_d \ , \\ 0 & \text{otherwise} \ , \end{cases}$$

and n_d denotes the number of calendar days passed since the beginning of the simulation. In the three cases studied here, the simulation starts at midday (12.00).

5.2.1 Short time simulation

Figure 2 shows the evolution of the temperature inside the concrete block during the first 24 hours. Only the top of the block is shown on the picture, for the heights $0.6 \leq x \leq 1$. The temperature does not vary in space for $x \leq 0.6$, so this part was excluded to make the picture clearer.

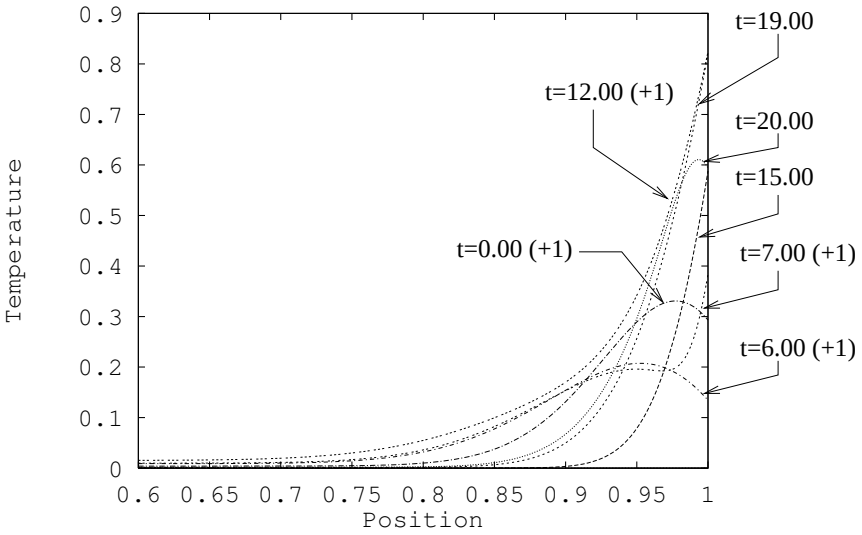

Figure 2: *Evolution of the temperature profile during the first 24 hours, here + denotes the following day.*

The initial temperature of the block is $T = 0$. Temperature profiles corresponding to times $t = 15.00, 19.00, 20.00, 0.00(+1), 6.00(+1), 7.00(+1), 12.00(+1)$ are shown on Figure 2. Here + denotes the following day. Two heating effects can be observed. The chemical reaction leads to a slow release of energy which acts to increase the temperature throughout the block. We can see at $x = 0.6$ that there is a very small rise in the temperature there. The boundary condition $\partial_x T = 0$, imposed at $x = 0$, prevents energy from leaving at that boundary. Hence, even though the hydration reaction is slow the temperature must slowly increase inside the block. In the vicinity of $x = 1$, we see the effect of the ambient temperature on the block. During day time solar radiation causes a significant rise in the temperature at the top of the block. This effect is balanced by the influence of ambient temperature. During the day, the ambient temperature is assumed to vary between $T_{min} = 288$K and $T_{max} = 303$K in dimensional form, corresponding to $T_{min} \sim -0.15$ and $T_{max} \sim 0.15$ in non-dimensional form. The surface temperature is well above $T = 0.15$ from the first hour so the ambient temperature cools the surface down. This effect is hard to notice during day time, but as soon as solar radiation stops, at 19.30, the temperature at $x = 1$ drops significantly. After 30 minutes without sun the non-dimensional drop in temperature (from the maximum value) is $\Delta T \approx 0.2$. Just before sunrise, at 06.00, the surface temperature has dropped to $T = 0.15$ from $T \approx 0.8$ the previous day at 19.00 of the previous day. When the sun rises again, the temperature increases more rapidly than on the previous day due to the residual heat in the block. At the end of the first 24 hours, it has reached $T = 0.8$, slightly above the maximum temperature observed the previous day, and will continue to increase as the day proceeds.

The heat gained at the surface slowly diffuses through the concrete block. In the first three hours the variations at the surface of the block only affect the temperature above $x = 0.9$ at first.

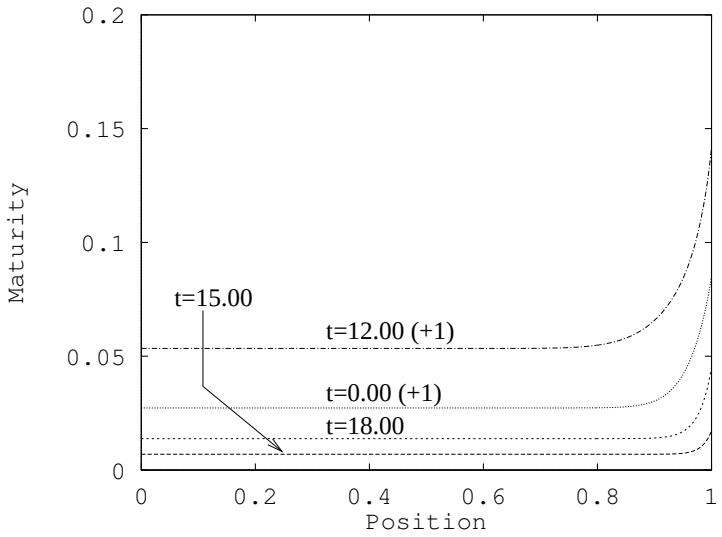

Figure 3: *Evolution of the maturity profile during the first 24 hours.*

Progressively, the effects may be seen up to $x = 0.7$ after one day. However, during the first day, most of the heat inside the block is released by the chemical reaction and heat diffusion is mainly observed at the top of the block.

The evolution of the maturity over the first 24 hours is shown in Figure 3. The maturity increases slowly over the first few hours. After a day, just over 5% of the concrete hydration has happened. This is also well predicted by the bulk solution (25). The reaction releases heat, causing the temperature rise as observed in Figure 2. The maturity is approximately constant throughout the block except near $x = 1$ where it is accelerated by the increase in surface temperature. Figure 4 shows the moisture variation. As the analytical solution suggests, the moisture variation is the opposite of the maturity, $\theta = 1 - \eta m$. The moisture level after a day is just about 95% of the initial value. Since the water is used in the hydration process it is nearly constant throughout the concrete block and only decreases at the top where the reaction is more advanced. Again the evolution is well modelled by the bulk solution (27)

5.2.2 Longer time simulation

The maturation process is now studied on a much longer term. The daily variations are still taken into account in the simulation but for comparison purposes, the variables will only be plotted at midday in the following two sections.

The variation of the maturity over the first two months may be seen in Figure 5. The trend observed in Figure 3 that the maturity is approximately constant through the bulk can still be seen, but as t increases the increase near $x = 1$ diffuses through the layer. After 60 days the maturity is close to its final value, $m = 0.8$ everywhere. It shows a very slight linear increase from $x = 0$ to

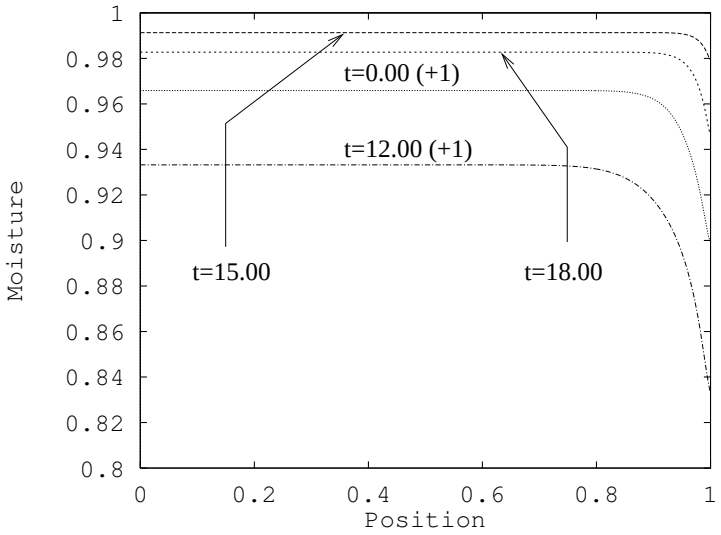

Figure 4: *Evolution of the moisture profile during the first 24 hours.*

around $x = 0.98$, followed by a small peak close to the boundary. This rise is due to some ambient moisture diffusing into the layer allowing the hydration reaction to continue at a very slow rate although all the initial moisture has been used.

In Figure 6 we compare the numerical and analytical solutions for maturity after 2 and 10 days. After 2 days, the constant analytical solution and the numerical solution are nearly equal over most of the layer, they only differ near $x = 1$ where the external energy has accelerated the reaction in the numerical solution. After 10 days, a lot of heat has been released in the layer due to the hydration reaction. The numerical solution also contains the external energy input and this extra energy has diffused through the block. The result is that the analytical solution differs from the numerical one by about 15% in the bulk and the correspondence deteriorates as the top of the block is approached. This result is in agreement with our earlier statement that the analytical solution will only hold for short time periods.

The moisture evolution is shown in Figure 7. The moisture slowly decreases throughout the block, but the decrease is most rapid near $x = 1$ where water is lost to the hydration reaction and evaporation. After 60 days we can see that for $x < 0.85$ there is a small amount of water remaining and the hydration can continue . For $x > 0.85$, the water has been used up and the reaction can therefore only continue close to $x = 1$ where some ambient water can diffuse in. Since diffusion is very slow this will slow the reaction down significantly. Hence, after 60 days both the maturity and moisture have almost reached their final limits.

The temperature evolution behaves in a very different manner. Temperature increase is due to the hydration reaction and energy gains or loss (at night) at the surface $x = 1$. The insulation condition at $x = 0$ prevents any heat loss there. Heat diffusion in concrete is very slow, the diffusion

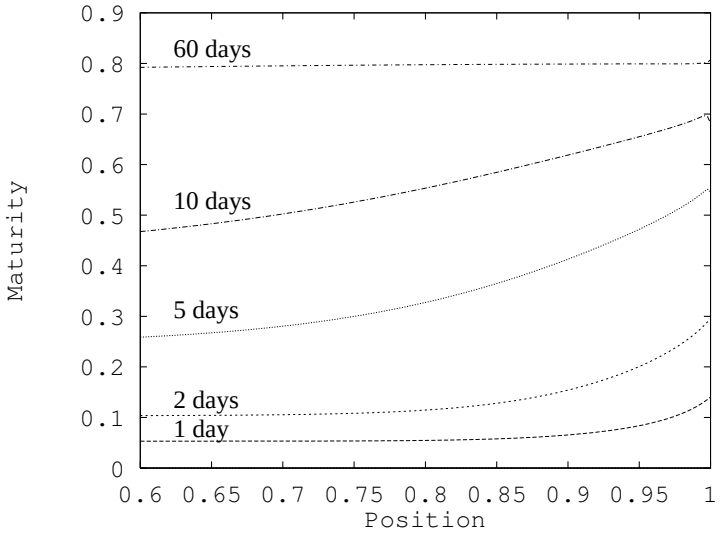

Figure 5: *Evolution of the maturity profile during the first 2 months.*

coefficient is $D_c = \kappa_c/\rho_c c_c \sim 10^{-6}\text{m}^2/\text{s}$. Consequently we see a slow temperature rise near $x = 0$. Near $x = 1$ the temperature remains high at the boundary and this can be seen to diffuse through the layer. As time increases, diffusion allows much of this energy to be spread through the layer. There will always be a boundary layer near $x = 1$ that reflects the daily variation, which does not have time to diffuse far.

5.2.3 Longer time simulation with two blocks

We now investigate the effect of adding a second block to the first one after 30 days. We begin by running the simulation for a single block for 30 days. We then place an identical block on top, with the same initial conditions as the original block. The boundary conditions at the surface specified at the start of this section remain valid. When the second block is added, they are applied at $x = 2$ instead of $x = 1$.

The maturity evolution is shown in Figure 9. A close up of the interface is shown in Figure 10. The initial block has a maturity increasing from 0.68 to approximately 0.78 near $x = 1$ after 30 days. At this stage the reaction could be expected to proceed very slowly, particularly near $x = 1$ where the maturity is close to the maximum, $m = 0.8$. The addition of the second block provides a new source of water for the first block. This water diffuses into the first block and the maturity then increases to around 0.9 after 60 days. This gain in water for the first block is a loss for the second, which results in a lower than expected maturity near the interface. After 60 days the minimum maturity, near $x = 1$, is around 0.62. Near the outer surface, $x = 2$, we can see the slight dip in maturity caused by the evaporation of water near the surface.

The corresponding moisture profiles are shown in Figures 11 and 12. In particular on Figure

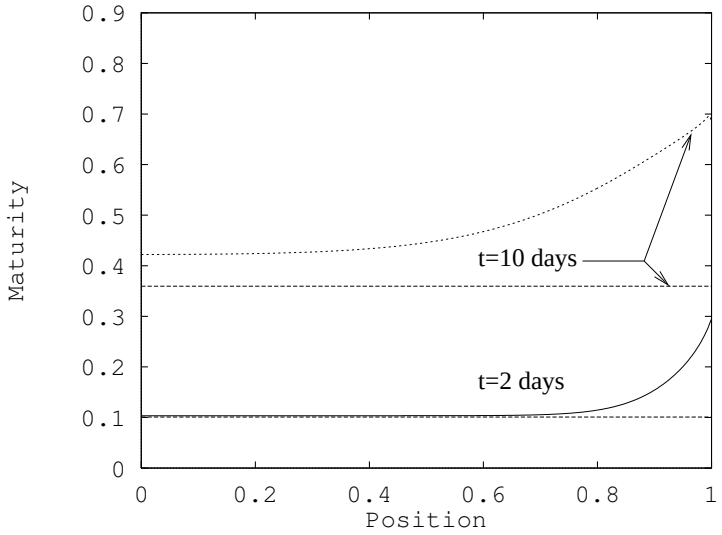

Figure 6: *Comparison of numerical and analytical maturity curves.*

12 we can see that after 30 days there is little water anywhere in the block. The addition of the second block increases the moisture considerably. After 60 days there is still a significant amount of water left in the second block, so we expect the reaction to continue for some time.

The temperature profile is shown in Figure 13. The addition of the second block insulates the first from the external energy and so we see the high temperature near $x = 1$ slowly diffuse through the block until after around 40 days. The temperature is then approximately constant for $x < 1$, the variation is all in the second block. We see the usual peaks near $x = 2$ due to the high midday temperatures. The central part of the second block is originally cool but rapidly heats up since it is heated from both sides. At the end of the simulation the temperature profile shows no indication of the two stage building.

5.2.4 Comparison between building a concrete block in a single or two stages

In the previous sections, we have based our simulations on the standard practice of building in 3 metre sections. We now compare the effects of building a 6 metre block in a single pour and by making it out of two 3 metre blocks. In Figures 14 and 15 we present the maturity and temperature after 60 days for this problem. As noted in the previous section the maturity at the top of the first block increases above its expected value at the expense of the upper block. Consequently there is a region where the maturity is well below the average value. When the block is completed in a single pour we see that the maturity in the lower region, $x < 1$ is below the two stage value, however for $x > 1$ it is higher and more importantly does not exhibit the weak spot (low maturity) at the join. The temperature curves show that the two stage process leads to a much hotter block. This is because our simulations are carried out at relatively high ambient temperatures. After the

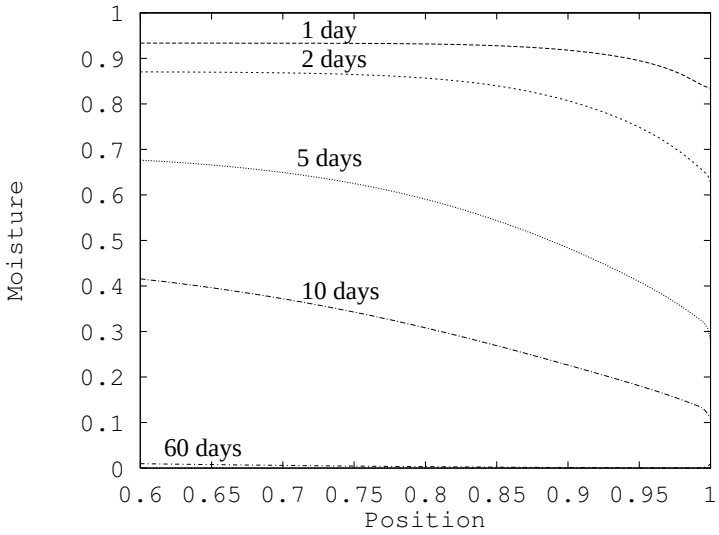

Figure 7: *Evolution of the moisture profile during the first 2 months.*

lower block is poured there are 30 days for the outside temperature to work into the block. The warm block is subsequently covered, insulating it from the outside, and the new block is heated. The single pour block is at a lower temperature since the lower regions are not exposed to so much external heat. We do not show the moisture profile since this can be inferred from the maturity.

These results appear to contradict accepted practice that it is better to build sequentially. This is perhaps related to the fact that our simulations are based on African temperatures. If we decrease the ambient temperature to emulate the standard frosty English weather, then the prime source of heat will be the concrete. In which case exposure to the air will aid in cooling rather than the heating seen from our calculations.

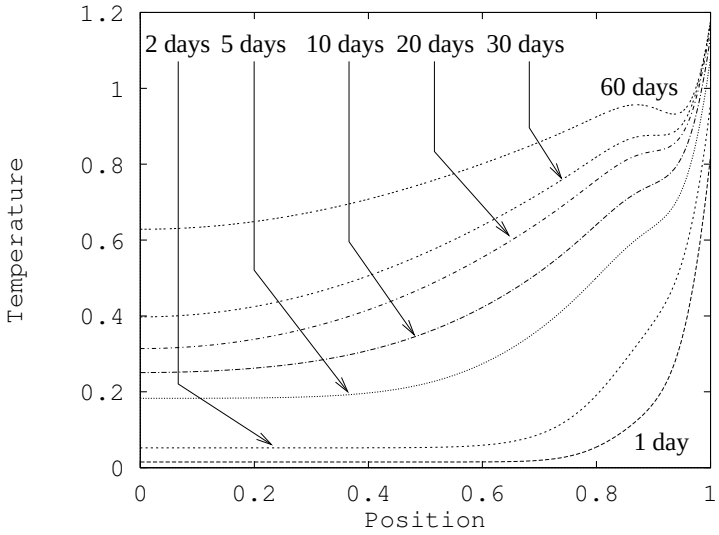

Figure 8: *Evolution of the temperature profile at 12.00 during the first 2 months.*

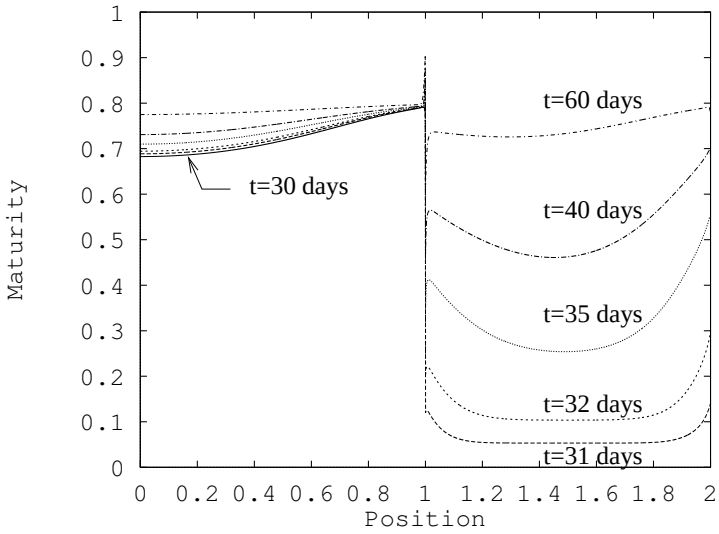

Figure 9: *Evolution of the maturity profile during the second month of a two layer simulation.*

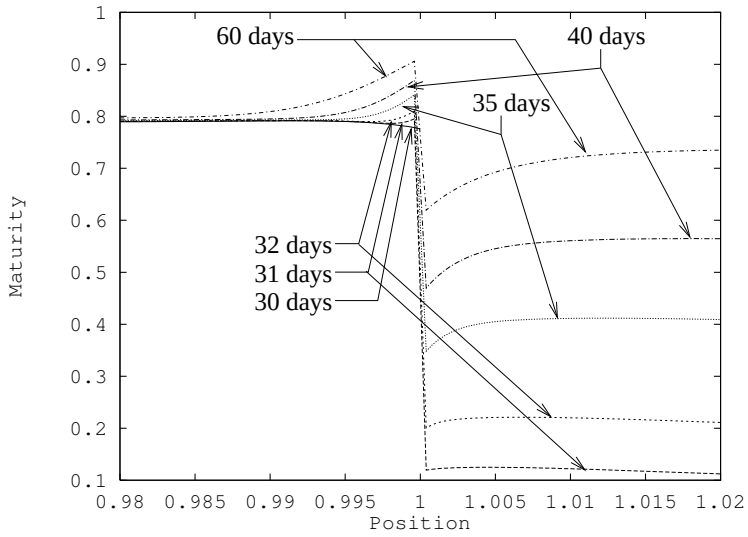

Figure 10: *Evolution of the maturity profile around the interface.*

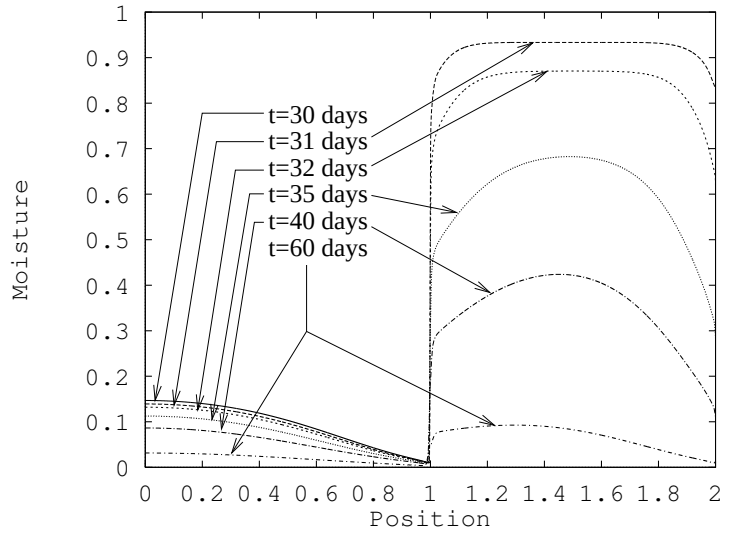

Figure 11: *Evolution of the moisture profile during the second month of a two layer simulation.*

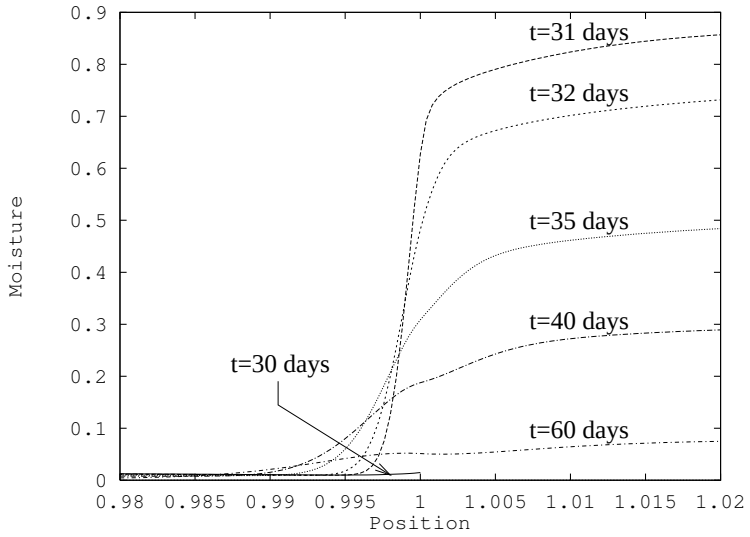

Figure 12: *Evolution of the moisture profile around the interface.*

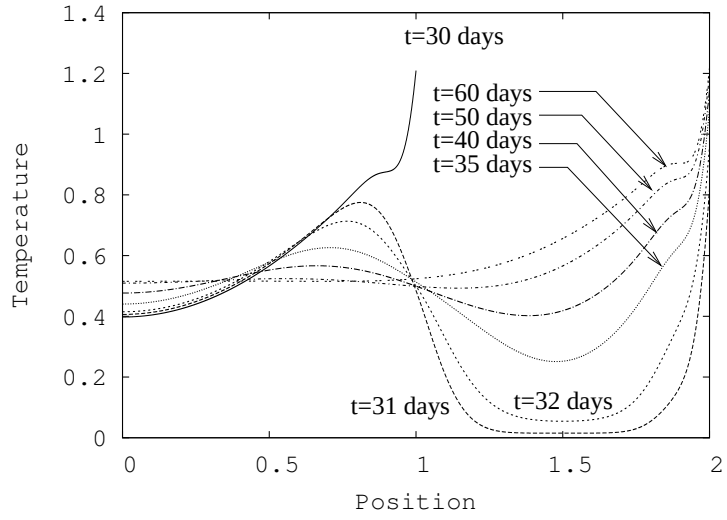

Figure 13: *Evolution of the temperature profile during the second month of a two layer simulation.*

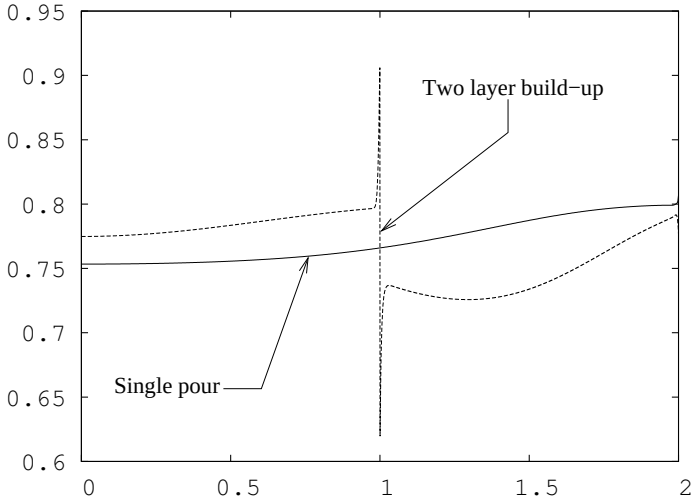

Figure 14: *Comparison of maturity profiles after two months for two build up methods.*

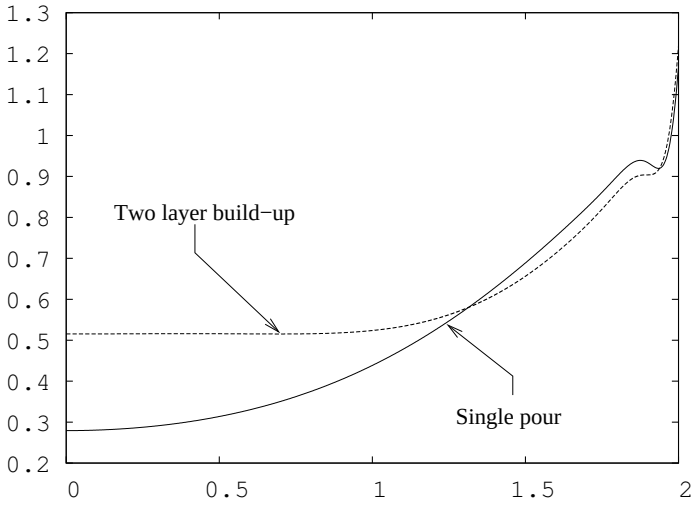

Figure 15: *Comparison of temperature profiles after two months for two build up methods.*

6 Conclusion

The main outputs of this work are the mathematical model of the maturation process and numerical scheme that can model the evolution of maturity, moisture and temperature of a concrete block through time. Results were presented for both short and long times.

A number of interesting features were observed in the calculations. For short times, of the order of days, the maturity increases most rapidly near the free surface. However, over a long period this surface will be the least mature, due to the fact that water evaporates and is not available for the reaction. Of course over even longer time periods it is possible that water from the atmosphere could permit the reaction to slowly continue. When a second block is added to the first then water can diffuse from the upper block to the lower one. This results in the top of the lower block becoming more mature than expected. The loss of water at the bottom of the upper block leads to a decrease in maturity there with a consequent effect on the concrete strength.

The graphs of moisture content showed that the free surface would always have a lower water content than the locations deeper down in the block. As discussed in the introduction, impervious floor coverings are often laid when measurements of the surface moisture indicate that the concrete is sufficiently dry. Our results show that the bulk moisture can be significantly higher than the surface value, at times by a factor of 2. When the covering is laid diffusion of the bulk water will raise the surface value and consequently lead to the damage described in [2].

The analytical model showed good agreement with the numerical results for small times. However, the neglect of diffusion prevented the inclusion of the surface boundary conditions. These clearly have a significant effect on the maturation process and the full numerical solution must be used for simulations lasting more than a few days.

A comparison of the difference between building a 6 metre block out of two 3 metre blocks or as a single pour gave surprising results. In the introduction we quote conventional wisdom, that cooling occurs at the free surface and so it is best to build sequentially. Our results show that the temperature within the block made in two sections was generally higher than that from the single pour. This can be attributed primarily to the fact that the simulations were carried out with the ambient temperature based on typical South African values, so a large amount of heat entered through the surface. In many countries, the free surface will act as a heat sink. The base may also have an effect on the result since this was insulated, when in reality it should act as a heat sink and cool down the lower region of the block. However, it is unclear whether this will have a greater effect on the single or two stage block. A cause of concern for sequential building is the jump in maturity at the interface. As discussed above, this leads to a weak spot in the concrete.

Perhaps the biggest drawback of the current model is the boundary condition at $x = 0$. Since this boundary could be in contact with a number of materials we chose an easy option, namely insulating the boundary. Heat and moisture could therefore only escape at the free surface and consequently the behaviour at the free surface played a more significant role than in reality. To

improve the model it will clearly be necessary to address this issue and presumably include some form of cooling condition, dependent upon the material below the initial block. This should be simple to implement numerically, particularly since we have already addressed the issue at the free surface, but would require a more specific case study, focussing on a given substrate.

7 Nomenclature

c_c	Thermal capacity of concrete	880	$\mathrm{J{\cdot}kg^{-1}{\cdot}K^{-1}}$
$\overline{e}$	Evaporation rate	1.8×10^{-9}	$\mathrm{m{\cdot}s^{-1}}$
m	Maturity	0-1	ND
m_x	Parameter for the hydration heat release	0.15	ND
t	Time		s
x	Cartesian coordinate		m
D_m	Moisture diffusivity in concrete	2×10^{-9}	$\mathrm{m^2{\cdot}s^{-1}}$
E	Apparent activation energy of the reaction	35×10^3	J
H	Heat transfer coefficient	5	$\mathrm{W{\cdot}K^{-1}{\cdot}m^{-2}}$
L	Length scale	3	m
Q_s	Heat received at the surface	500	$\mathrm{J{\cdot}m^{-2}{\cdot}s^{-1}}$
Q_x	Parameter for the hydration heat release	10^8	$\mathrm{J{\cdot}m^{-3}}$
R	Gas constant	8.314	$\mathrm{J{\cdot}K^{-1}}$
T	Non-dimensional temperature	0-1	ND
T_s	Initial temperature	295.5	K
ΔT	Typical temperature jump in the block	48.3	K
α_1	$\kappa_c \tau/(\rho_c c_c L^2)$	0.015	ND
α_2	$D_m \tau/(L^2)$	4.6×10^{-5}	ND
η	Stoichiometric ratio for the hydration reaction	1.25	ND
θ	Moisture content	0-1	ND
θ_a	Ambient moisture content	0.05	ND
θ_s	Initial moisture content	1	ND
κ_c	Specific heat capacity	1.37	$\mathrm{W{\cdot}K^{-1}{\cdot}m^{-1}}$
λ	$E\rho_c c_c/[R\,(Q_x + \rho_c c_c T_s)]$	12.2	ND
μ	Reaction rate	1	$\mathrm{s^{-1}}$
ρ_c	Density of concrete	2350	$\mathrm{kg{\cdot}m^{-3}}$
τ	Time scale	2.08×10^5	s

Acknowledgements

J.C. acknowledges the support of the Mathematics Applications Consortium for Science and Industry (MACSI), under the auspices of the Science Foundation of Ireland (SFI) Mathematics initiative.

References

[1] Pavlik J., Tydlitat V., Cerny R., Klecka T., Bouska P., Rovnanikova P. Application of a microwave impulse technique to the measurement of free water content in early hydration stages of cement paste. Cement & Concrete Research 33: 93-102, 2003. 25

[2] West R.P., Holmes N. Predicting moisture movement during the drying of concrete floors using finite elements. Construction & Building Materials 19 (9): 674-681, 2005. 25, 26, 27, 46

[3] Ballim Y. and Graham P.C. A maturity approach to the rate of heat evolution in concrete. Magazine of Concrete Research 55(3) (2003) 249-256. 26

[4] Charpin J.P.F., Myers T.G., Sjöberg A. & Ballim Y. Modelling the temperature, maturity and moisture content in a drying concrete block. Proc. 3rd Mathematics in Industry Study Group South Africa (MISGSA2006), University of the Witwatersrand 25, 26

[5] Fowkes N.D., Mamboundou H.M., Makinde O.D., Ballim Y. & Patini A. Maturity effects in concrete dams. Proc. Mathematics in Industry Study Group South Africa (MISGSA2004), University of the Witwatersrand, pp 59-67, 2004. 25

[6] Cement & Concrete Institute website. http://cnci.org.za/default.htm. Last time accessed 14/5/2008. 25, 27

[7] Charpin J.P.F., Myers T.G., Fitt A.D., Ballim Y. & Patini A. Modelling surface heat exchanges from a concrete block into the environment. Proc. Mathematics in Industry Study Group South Africa (MISGSA2004), University of the Witwatersrand, pp 51-58, 2004. 25, 27

[8] US Bureau of Reclamation, Hoover Dam: Concrete, http://www.usbr.gov/lc/ hoover-dam/History/essays/concrete.html, last accessed 14/5/2008. 25

[9] Myers T.G., Fowkes N.D. & Ballim Y. A mathematical analysis of the effect of piped water cooling in concrete. Submitted to ASCE J. Engng Mech., Feb. 2008. 25, 26